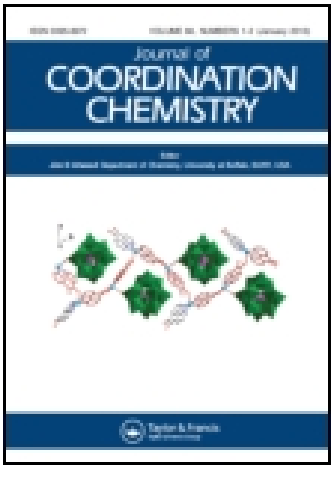

Journal of Coordination Chemistry
Publication details, including instructions for authors and subscription information:
http://www.tandfonline.com/loi/gcoo20

Self-activated DNA cleavage of a water-soluble mononuclear Cu(II) complex with polyquinolinyl ligand

Jun-Ling Li[abd], Lin Jiang[abc], Si-Tong Li[abc], Jin-Lei Tian[abcd], Wen Gu[ab], Xin Liu[abc] & Shi-Ping Yan[ab]

[a] Department of Chemistry, Nankai University, Tianjin, PR China

[b] Tianjin Key Laboratory of Metal and Molecule Based Material Chemistry, Tianjin, PR China

[c] Key Laboratory of Advanced Energy Materials Chemistry (MOE), Tianjin, PR China

[d] Collaborative Innovation Center of Chemical Science and Engineering, Tianjin, PR China

Accepted author version posted online: 13 Oct 2014.Published online: 29 Oct 2014.

To cite this article: Jun-Ling Li, Lin Jiang, Si-Tong Li, Jin-Lei Tian, Wen Gu, Xin Liu & Shi-Ping Yan (2014) Self-activated DNA cleavage of a water-soluble mononuclear Cu(II) complex with polyquinolinyl ligand, Journal of Coordination Chemistry, 67:22, 3598-3612, DOI: 10.1080/00958972.2014.973867

To link to this article: http://dx.doi.org/10.1080/00958972.2014.973867

Journal of Coordination Chemistry, 2014
Vol. 67, No. 22, 3598–3612, http://dx.doi.org/10.1080/00958972.2014.973867

Self-activated DNA cleavage of a water-soluble mononuclear Cu(II) complex with polyquinolinyl ligand

JUN-LING LI†‡¶, LIN JIANG†‡§, SI-TONG LI†‡§, JIN-LEI TIAN*†‡§¶, WEN GU†‡, XIN LIU*†‡§ and SHI-PING YAN†‡

†Department of Chemistry, Nankai University, Tianjin, PR China
‡Tianjin Key Laboratory of Metal and Molecule Based Material Chemistry, Tianjin, PR China
§Key Laboratory of Advanced Energy Materials Chemistry (MOE), Tianjin, PR China
¶Collaborative Innovation Center of Chemical Science and Engineering, Tianjin, PR China

(*Received 30 June 2014; accepted 17 September 2014*)

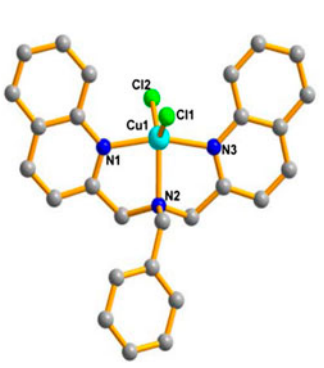

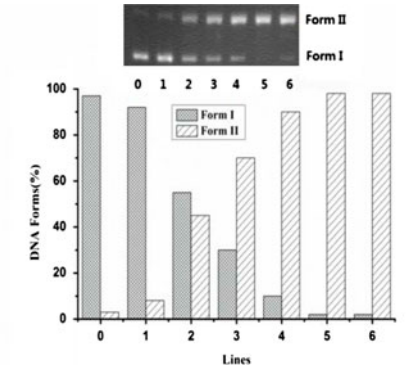

The synthesis and characterization of a water-soluble mononuclear Cu(II) complex, [Cu**L**Cl_2]·2CH_3-CH_2OH, where **L** = bis(2-quinolinyl methyl)benzyl-amine has been reported. **L** is a tridentate polyquinolinyl ligand, coordinated to Cu(II) via NNN donors. The central copper ion of **1** has N_3Cl_2 donor set in a distorted trigonal-bipyramidal geometry. The dimer existing in the solid state resulted from hydrogen bonds and π–π accumulation between two mononuclear units. The interaction of **1** with CT-DNA has been explored by absorption and emission titration methods, revealing partial intercalation between **1** and CT-DNA. Moreover, **1** could make pBR322 plasmid DNA cleaved by a self-activated oxidative process; hydroxyl radical and singlet oxygen may be the main reactive oxygen species species in the process. Complex **1** may quench the intrinsic fluorescence of bovine serum albumin in a static quenching process, which has been investigated by UV–visible and fluorescence spectroscopic methods. **1** also demonstrates potent cytotoxity against Hela cells with IC_{50} value of 2.84 μM, which shows it to be a potential candidate as an anticancer metal-based drug.

Keywords: Cu(II) complex; Water soluble; Self-activation DNA cleavage; Protein binding

*Corresponding authors. Email: tian@nankai.edu.cn (J.-L. Tian); liuxin64@nankai.edu.cn (X. Liu)

1. Introduction

Metal complexes constitute an important class of compounds with biological interest [1]. In 1964, the observation of cis-$[Pt(NH_3)_2Cl_2]$ prompted a growing interest in the development of metal-based drugs to suppress cell division and clinical use for treatment of cancers [2]. The platinum family, carboplatinum, and oxaliplatin have been used in clinical studies. Recently, two ruthenium complexes, NAMI-A, [ImH][trans-$RuCl_4$(DMSO)(Im)] (where Im = imidazole) and KP1019, [InH][trans-$RuCl_4(In)_2$] (where In = indazole) have entered clinical trials [3]. Transitional metal complexes have also attracted attention for its two advantages as DNA-binding agents [4]: (i) well-defined coordination geometries to provide attractive moieties for reversible recognition of nucleic acids; and (ii) distinctive electrochemical or photophysical properties thus enhancing the functionality of a binding agent.

Copper is an essential element for most aerobic organisms, so Cu-based complexes have been investigated on the assumption that endogenous metals may be less toxic for normal cells than cancer cells [5–8]. Recently, Carlo Santini and his co-workers have elaborated on the advances of copper-based complexes as anticancer drugs [9]. Moreover, Kaushik Ghosh *et al.* investigated a mononuclear Cu(II) complex, which shows self-activated DNA cleavage and affords excellent anticancer activity against MCF-7 cells. A ternary copper–terpyridine complex, $[Cu(ttpy)(Gly)(NO_3)](NO_3)\cdot H_2O$ (ttpy = 4′-p-tolyl-2,2′:6,2″-terpyridine, Gly = glycine), also displays remarkable DNA cleavage activity in the presence of Vc [10]. As neutral, non-deprotonated chelating ligands, di(picolyl)amine (dpa) and its derivatives form many complexes, some of which show efficient DNA binding, cleavage activity, as well as anticancer activities [11]. Especially, with N-benzyl di(pyridylmethyl)amine (phdpa), Cu(II) complexes could effectively inhibit the proliferation of cancer cells, A549, Hela and HepG-, with IC_{50} values lower than 5-Fluorouracil [12]. Compared with pyridine, quinoline ring shows better planarity and stronger hydrophobic DNA interaction, which may enhance DNA binding ability [6]. In addition, quinoline and its derivatives could be a privileged scaffold in cancer drug discovery [13]. So, it will be interesting to investigate biological activities of Cu(II) complexes with quinoline substituted di(picolyl)amines ligands.

A mononuclear Cu(II) complex, $[Cu\mathbf{L}Cl_2]\cdot 2CH_3CH_2OH$, where **L** = bis(2-quinolinyl methyl)benzyl-amine, has been synthesized and structurally characterized. Complex **1** shows good water solubility, which provides a good start for further investigations. After investigations of interaction between **1** and DNA by different techniques, **1** not only efficiently binds with CT-DNA, but also reveals self-activated oxidative DNA cleavage. Moreover, **1** also could quench the intrinsic fluorescence of bovine serum albumin (BSA) in a static quenching process. Complex **1** also demonstrates potent cytotoxicity against Hela cells with IC_{50} of 2.84 μM.

2. Experimental

2.1. *Materials and measurements*

All reagents and chemicals were purchased from commercial sources and used as received. Plasmid pBR322 DNA, agarose, ethidium bromide (EB), BSA, glutathione monoester (GSH-OEt), and calf thymus CT-DNA were obtained from Sigma. Stock solutions of **1** (1.0×10^{-3} M in H_2O) were stored at 4 °C and prepared to required concentrations for all

experiments. Ultra-pure MilliQ water (18.24 MΩ cm) was used in all experiments. Tris–HCl and phosphate buffer solution were prepared using ultrapure water. Cell counting kit-8 (CCK-8) was purchased from Dojindo Molecular Technologies, Inc. Elemental analyses for C, H, and N were obtained on a Perkin-Elmer analyzer model 240. Infrared spectra on KBr pellets were performed on a Bruker Vector 22 FT-IR spectrophotometer from 4000 to 400 cm^{-1}. Electrospray ionization mass spectrometry was obtained on an Agilent 6520 Q-TOF LC/MS. Electronic spectra were measured on a JASCO V-570 spectrophotometer. Fluorescence spectral data were obtained on a MPF-4 fluorescence spectrophotometer at room temperature. The gel imaging and documentation DigiDoc-It System was assessed using Labworks Imaging and Analysis Software (UVI, UK).

2.2. *Synthesis of L and 1*

2.2.1. Preparation of ligand. L (scheme 1) was prepared according to a procedure described in the literature [14] with some improvements. A mixture of 2-chloromethylquinoline hydrochloride (1.82 g, 8.4 mM), benzylamine (0.45 g, 4.2 mM), and potassium carbonate (3.5 g, 26 mM) in acetonitrile (30 mL) was refluxed for 48 h. After the solvent was removed under reduced pressure, the residue was separated by chloroform/water and the organic phase was dried, evaporated, and pale yellow powder was obtained, yield 1.05 g (64%). Selected IR data (KBr, *v*, cm^{-1}): 3415(s), 3328(w), 1638(s), 1617(s), 1504(w), 1426 (w), 1117(m), 824(m), 766(w), 620(s), 482(m), 411(w). ^{1}H NMR ($CDCl_3$): δ(ppm) 8.12 (2H, d), 8.05 (2H, d), 7.79 (2H, t), 7.74 (2H, d), 7.67 (2H, m), 7.50 (2H, m), 7.44 (2H, d), 7.32 (2H, m), 7.23 (1H, m), 4.02 (4H, s), 3.73 (2H, s).

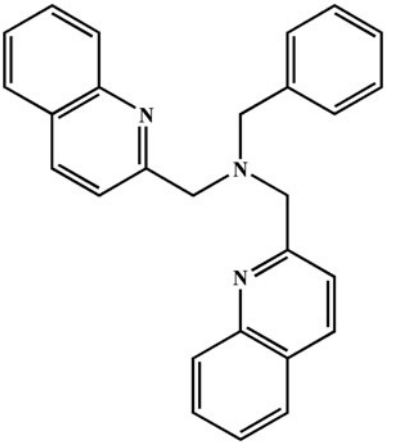

Scheme 1. Schematic structure of **L**.

2.2.2. Synthesis of $[CuLCl_2]\cdot 2CH_3CH_2OH$. To an ethanol solution (10 mL) of **L** 0.0392 g (0.1 mM), an aqueous solution (5 mL) of $CuCl_2\cdot 2H_2O$ 0.0172 g (0.1 mM) was added. The resulting mixture was stirred for 3 h at room temperature. Cyan prism crystals suitable for X-ray diffraction were obtained by slow evaporation of the filtrate after 15 days, which were collected by filtration, washed with diethyl ether, and dried in air, yield

0.0137 g (22%). Elemental analysis (%): Anal Calcd for $C_{31}H_{35}Cl_2CuN_3O_2$: C, 60.44; H, 5.73; N, 6.82. Found: C, 60.58; H, 5.62; N, 6.89. Selected IR data (KBr, ν, cm^{-1}): 3415(s), 3328(w), 2026(m), 1638(s), 1617(s), 1456(w), 1129(m), 623(s), 484(m), 410(w).

2.3. *X-ray crystallographic studies*

Single-crystal X-ray diffraction data were collected on a Bruker Smart 1000 CCD diffractometer using Mo K_α radiation (λ = 0.71073 Å) with the ω scan technique. The structure of **1** was solved by direct methods (SHELXS-97 and refined with full matrix least squares on F^2 using SHELXL-97 [15]). The hydrogens were added theoretically, riding on the concerned atoms and refined with fixed thermal factors. The details of crystallographic data and structure refinement parameters are summarized in table 1, and selected bond angles and distances are listed in table 2. Crystallographic data for **1** have been deposited with the Cambridge Crystallographic Data Center with the corresponding CCDC reference number of 997352.

Table 1. Crystal data and structure refinement for **1**.

Compound reference	Complex
Chemical formula	$C_{31}H_{35}Cl_2CuN_3O_2$
Formula mass	616.06
T (K)	113.15
Crystal system	Monoclinic
Space group	$P2(1)/n$
a (Å)	9.2716(19)
b (Å)	15.010(3)
c (Å)	20.722(4)
α (°)	90.00
β (°)	97.45(3)
γ (°)	90.00
V (Å^3)	2859.4(10)
No. of formula units per unit cell (Z)	4
Radiation type	Mo/Kα
Absorption coefficient (μ/mm^{-1})	0.985
No. of reflections measured	26,792
No. of independent reflections	5037
R_{int}	0.0469
Final R_1 values [$I > 2\sigma(I)$]	0.0438
Final $wR(F^2)$ values [$I > 2\sigma(I)$]	0.1180
Final R_1 values (all data)	0.0494
Final $wR(F^2)$ values (all data)	0.1219

Table 2. Selected bond lengths (Å) and angles (°) for **1**.

Cu(1)–N(3)	1.988(2)	Cu(1)–Cl(2)	2.3277(9)
Cu(1)–N(1)	1.994(2)	Cu(1)–Cl(1)	2.4266(9)
Cu(1)–N(2)	2.137(2)		
N(3)–Cu(1)–N(1)	163.38(10)	N(2)–Cu(1)–Cl(2)	123.21(7)
N(3)–Cu(1)–N(2)	82.10(10)	N(3)–Cu(1)–Cl(1)	93.58(7)
N(1)–Cu(1)–N(2)	81.62(10)	N(1)–Cu(1)–Cl(1)	93.99(7)
N(3)–Cu(1)–Cl(2)	93.73(7)	N(2)–Cu(1)–Cl(1)	105.68(7)
N(1)–Cu(1)–Cl(2)	92.41(7)	Cl(2)–Cu(1)–Cl(1)	131.11(3)

2.4. *DNA binding and cleavage activity studies*

The UV absorbance at 260 and 280 nm of the CT-DNA solution in 5 mM Tris–HCl/50 mM NaCl buffer (pH 7.2) gives a ratio of 1.8–1.9, indicating that CT-DNA was sufficiently free of protein [16]. The concentration of CT-DNA was determined from its absorption intensity at 260 nm with a molar extinction coefficient of 6600 M^{-1} cm^{-1}. The absorption spectra of **1** binding to DNA were performed by increasing amounts of CT-DNA to **1** in Tris–HCl buffer (pH 7.2).

The relative binding abilities of **1** to CT-DNA were studied with an EB-bound CT-DNA solution in 5 mM Tris–HCl/50 mM NaCl buffer (pH 7.2). The fluorescence spectra were recorded at room temperature with excitation at 510 nm and emission at 602 nm. The experiments were carried out by titrating complex into EB-DNA solution containing 2.4×10^{-6} M EB and 48×10^{-6} M CT-DNA.

The DNA cleavage experiments were carried out by agarose gel electrophoresis, which was performed by incubating at 37 °C; pBR322 DNA (0.1 μg/μL) in 50 mM Tris–HCl 18 mM NaCl buffer (pH 7.2) was treated with complex. The samples were incubated for 3 h and loading buffer was added. Then the samples were electrophoresed for 2 h at 0.9% agorose gel using Tris–boric acid–EDTA buffer. After electrophoresis, bands were visualized by UV light and photographed.

Cleavage mechanism of pBR322 DNA was investigated in the presence of some radical scavengers and reaction inhibitors. The reactions were conducted by adding standard radical scavengers, KI, L-His, scavenger superoxide dismutase (SOD), EDTA, catalase, and groove binding agents – Methyl Green (for major groove) and SYBR Green (for minor groove) to pBR322 DNA after the addition of complex. Cleavage experiment was initiated by addition of complex and quenched with 2 μL of loading buffer. Further analysis was carried out by the above standard method.

2.5. *Protein binding studies*

Fluorescence quenching experiments have been carried out to investigate the interaction between BSA and **1** by using bovine serum albumin stock solution (BSA, 1.5 mM) in 10 mM phosphate buffer (pH 7.0). The fluorescence spectra were recorded at room temperature with excitation of BSA at 280 nm and emission at 342 nm by keeping concentration of BSA constant (29.4 μM) while varying the complex concentration from 0 to 40 μM.

2.6. In vitro *cell assay*

The cytotoxicity assay of **1** against Hela cervical carcinoma cells was evaluated by a CCK-8 kit assay. The Hela cells were cultured in a DMEM/F12 medium supplemented with 10% fetal bovine serum (5% CO_2 at 37 °C). The cells were seeded into 96 well plates at a density of 10^4 cell/well and incubated for 48 h to allow cell attachment. Then, the cells were washed with PBS, and the medium was replaced with a fresh medium containing the indicated concentrations of **1**. Cells without pretreatment were used as the control. After a period of incubation, the cells were washed with PBS and incubated in DMEM/F12 with 10% WST-8 solution for another 2 h. The absorbance of each well was measured at a wavelength of 450 nm with a plate reader. The results were expressed as the mean values of three measurements. The cell viability was calculated as follows,

$$\text{cell viability}\,(\%) = \frac{I_{\text{sample}} - I_{\text{blank}}}{I_{\text{control}} - I_{\text{blank}}} \times 100$$

where I_{sample}, I_{control}, and I_{blank} represent the absorbance intensity at 450 nm determined for cells treated with different samples, for control cells (nontreated), and for blank wells without cells (the same amounts of the CCK-8 solution and the sample solution as the sample wells were added to the blank wells), respectively.

3. Results and discussion

3.1. *Description of the crystal structure*

The complex has been structurally characterized by X-ray crystallography (figure 1); details of the data collection conditions and the parameters of refinement are given in table 1, and selected bond lengths and angles are given in table 2.

Complex **1** crystallized in the monoclinic *P2(1)/n* space group with five-coordinate Cu with the N_3Cl_2 donor set is derived from one tertiary amine, two quinoline nitrogens, and two chlorides. The τ value of Cu is 0.54, which indicates that the geometry of **1** is distorted trigonal-bipyramidal. The basal plane is occupied by Cl(1), Cl(2), and N(2), while two quinoline nitrogens occupy the axial positions, with Cu–N distance (Cu–N(1) 1.994(2) Å, Cu–N(3) 1.988(2) Å) shorter than the equatorial distance (Cu–N(2) 2.137(2) Å). The bond distances of Cu–N and Cu–Cl (Cu–Cl(1) 2.4266(9) Å, Cu–Cl(2) 2.3277(9) Å) fall in the range of several reported Cu(II) complexes, $[Cu(L6)Cl_2]$(L6 = 2-(1H-benzimidazol-2-yl) ethyl-(4,4adihydroquinolin-2-ylmethylene)amine) [6] ($Cu–N_{imine}$ 2.050(2) Å, $Cu–N_{bzim}$

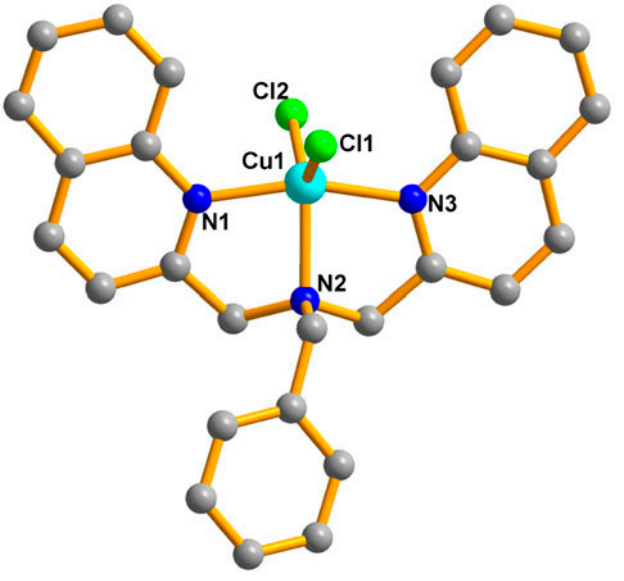

Figure 1. Molecular structure of **1**. Hydrogens and solvent molecules have been omitted for clarity.

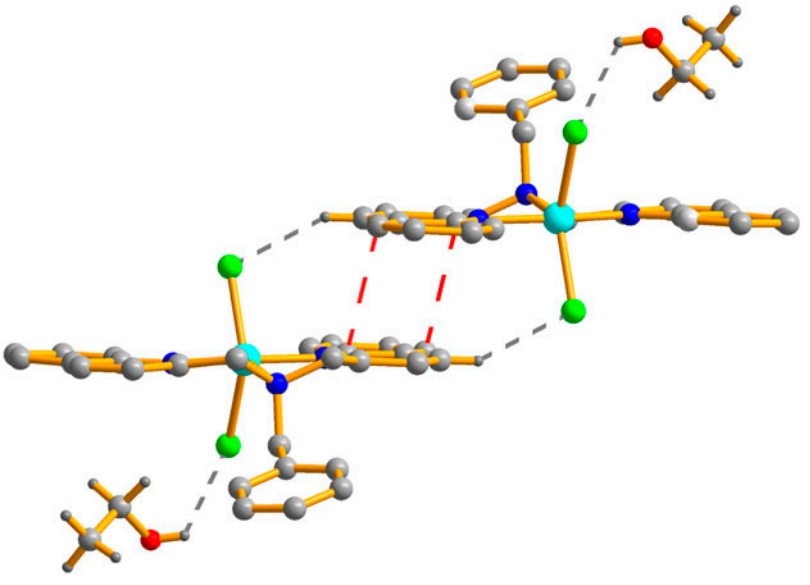

Figure 2. Depiction of interactions between hydrogen bonds in **1**.

1.972(2) Å, Cu–N_{quin} 2.041(2) Å, Cu–Cl(1) 2.360(8) and Cu–Cl(2) 2.354(7) Å) and $[CuCl_2(C_{12}H_{14}N_4)(H_2O)]$ ($C_{12}H_{14}N_4$ = {(1-methyl imidazol-2-yl)methylene}-2-amino ethyl-pyridine) [17] (Cu–N1 2.053(2) Å, Cu–N2 2.032(2) Å, Cu–N3 2.035(2) Å, Cu–Cl1 2.538(1) Å, and Cu–Cl2 2.302(1) Å).

A dimer exists between two mononuclear units in the solid state, which results from hydrogen bonds and π–π accumulation. Hydrogen bonds between the equatorial Cl^- ligand and O atom of ethanol, C atom of quinoline ring are presented in structure (figure 2). The respective bond distance and angles are listed in table 3. In O–H…Cl, the corresponding bond distances are similar with $[CuCl_2(C_{12}H_{14}N_4)(H_2O)]$ [17]. The bond distances in C–H…Cl also fall in the range of $[Cu_2(L8)(Cl)_4]$ (L8 = 1,4-bis[di(2-picolyl)aminomethyl]benzene) [18]. The hydrogen bonding between quinoline ring and coordinated Cl^- is further stabilized by aromatic π–π stacking interactions between two monomer units of quinoline rings with a center-to-center distance of 3.257 Å.

3.2. *DNA-binding and cleavage activities*

3.2.1. Absorption spectra studies. Electronic absorption spectroscopy is a common method to investigate the interaction between complex and DNA. If the compound binds to DNA through intercalation, hypochromism with or without a small red shift occurs, due to

Table 3. Hydrogen bonds (Å) and (°) of **1**.

D–H…A	*d*(D–H)	*d*(H…A)	*d*(D…A)	*θ*(∠DHA)
O1–H1…Cl1	0.82	2.873	3.266	111.68
C14#–H14#…Cl2	0.93	2.853	3.669	147.07

Note: #, 1−*x*, 2−*y*, −*z*.

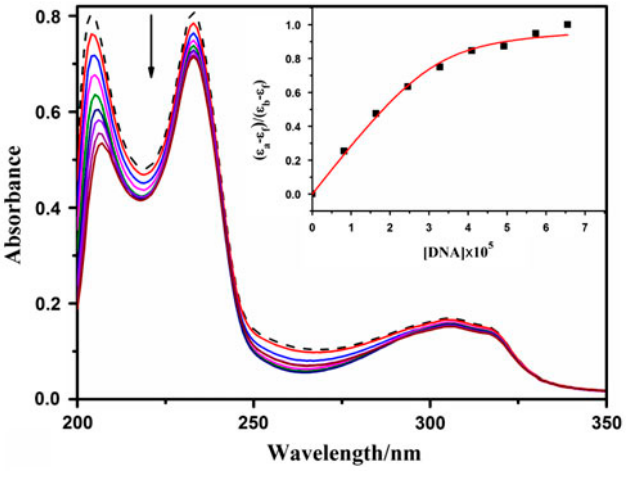

Figure 3. Absorption spectra of **1** in the absence (dashed line) and presence (solid line) of increasing amounts of CT-DNA (9.4–75.2 μM) in 5 mM Tris-HCl/50 mM NaCl buffer (pH 7.2). The insert shows the least-squares fit of $(\varepsilon_a-\varepsilon_f)/(\varepsilon_b-\varepsilon_f)$ *vs.* [DNA] for **1**.

stacking between the planar aromatic chromophore and the base pair of DNA [19, 20]. From figure 3, upon incremental addition of DNA to complex, the obvious decrease in molar absorptivity was observed, without a red shift, which is similar to several reported complexes [6]. In the presence of DNA, the absorption band of **1** exhibited a hypochromism about 11.7%. The result suggests that **1** may bind to DNA via intercalation. In order to determine the binding strength of **1** with CT-DNA, intrinsic binding constant K_b was calculated from a nonlinear fitting according to equations (1a) and (1b) [21].

$$(\varepsilon_a-\varepsilon_f)/(\varepsilon_b-\varepsilon_f)=\left(b-\left(b^2-2K_b{}^2C_t[DNA]/s\right)^{1/2}\right)/2K_bC_t \quad (1a)$$

$$b=1+K_bC_t+K_b[DNA]/2s \quad (1b)$$

Table 4. Absorption spectral properties and fluorescence spectral properties of **1** bound to CT-DNA.

Complex	K_b (M^{-1})	K_{app} (M^{-1})	Ref.
Complex **1**	9.18×10^5	1.06×10^6	This work
[(phdpa)Cu(bpy)(ClO_4)]		3.69×10^4	12
[(phdpa)Cu(phen)(H_2O)]		8.20×10^4	12
[Cu(L^3)Cl_2]		3.40×10^4	6
[Cu(L^6)Cl_2]	6.60×10^3	7.60×10^4	6
[$CuCl_2$(OQsc-H)]·H_2O·CH_3OH	$2.98(\pm0.13)\times10^5$	$2.91(\pm0.23)\times10^5$	19

Notes: Phdpa: N-benzyl di(pyridylmethyl)amine.
bpy: 4,4-dimethyl-2,2-bipyridine.
phen: 1,10-phenanthroline.
L^3: (2-pyridin-2-yl-ethyl)pyridin-2-ylmethyleneamine.
L^6: 2-(1H -benzimidazol-2-yl)ethyl-(4,4a-dihydroquinolin-2-ylmethylene)amine.
OQsc-H: 2-oxo-1,2-dihydroquinoline-3-carbaldehyde semicarbazone.

The DNA binding constant (K_b) of **1**, along with the binding site size (s), is given in table 4. The K_b value of **1** is 9.18×10^5 M^{-1}, which is larger than several reported mononuclear Cu(II) complexes [6, 19]. However, the K_b value is smaller than $[Cu(L^1)Br_2]$ (3.45×10^6 M^{-1}) (L^1 = (2-((quinolin-8-ylimino)methyl)pyridine)) [22], which may be due to the larger steric hindrance as a result of phenyl in **L**. The s value of **1** is 1.06, which may be due to an aggregation of hydrophobic molecules on the DNA surface by π stacking [23]. The DNA binding propensity is also determined from other assays.

3.2.2. Fluorescence spectral studies. Compound **1** shows no luminescence at room temperature in aqueous solutions. As a result, the EB–DNA system was used to further investigate the interaction between **1** and DNA. Emission spectra of EB bound to CT-DNA in the absence and presence of **1** are predicted in figure 4. As the concentration of complex increases, the emission band at 603 nm exhibited hypochromism up to 42.3% of the initial fluorescence intensity. The remarkable reduction in the emission intensity clearly indicates that EB molecules are replaced by **1** and released into solution [24]. Quenching data were analyzed according to the Stern–Volmer equation: $I_0/I = K_q[Q] + 1$, where I_0 and I represent fluorescence intensities in the absence and presence of quencher and $[Q]$ is the quencher concentration. In the linear fit plot of I_0/I *versus* $[Q]$, K_q is the Stern–Volmer dynamic quenching constant. The apparent DNA binding constant (K_{app}), which could express the degree of affinity toward DNA, was calculated on the basis of the equation,

$$K_{EB}\,[EB] = K_{app}\,[complex]$$

Here, $K_{EB} = 1.0 \times 10^7$ M^{-1} ([EB] = 2.4 μM). K_{EB} is the binding constant of EB to DNA and the complex concentration is the value at 50% reduction of the fluorescence intensity of EB. The K_{app} value of **1** is 1.06×10^6 M^{-1}, which is smaller than K_{EB} (1.0×10^7 M^{-1})

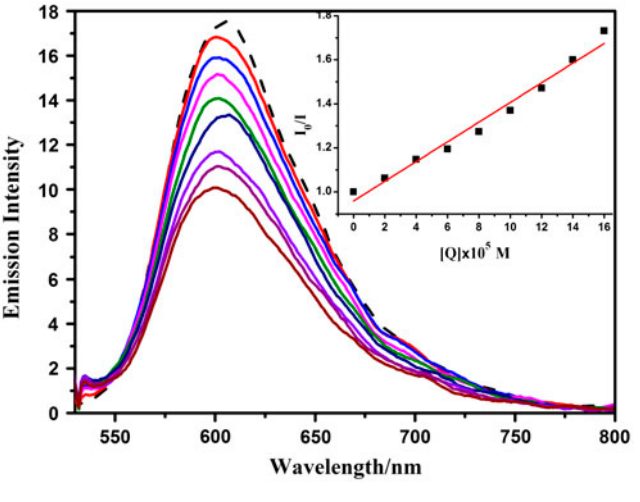

Figure 4. Emission spectra of EB bound to CT-DNA in the absence (dashed line) and presence (solid lines) of **1** (0–160 μM) in 50 mM Tris–HCl/18 mM NaCl buffer (pH 7.2). Inset: the plot of I_0/I *vs.* the complex concentration.

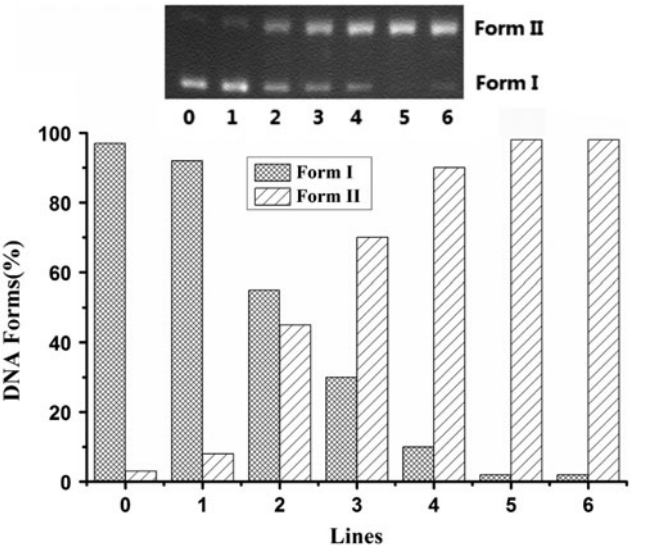

Figure 5. Cleavage of plasmid pBR322 DNA (0.1 μg/μL^{-1}) at different concentration of **1** after 3 h incubation at 37 °C; Line 0: DNA control; Lines 1–6: DNA + complex (5, 20, 25, 30, 35, and 40 μM).

and suggests moderate interactions between **1** and DNA. However, the value is higher than two Cu(II) complexes with similar structures [6] (table 4), $[Cu(L^3)Cl_2]$ (3.40×10^4 M^{-1}) and $[Cu(L^6)Cl_2]$ (7.60×10^4 M^{-1}), which suggests stronger DNA affinity than the two complexes. The result may indicate that ligand plays the main role in interaction with DNA. Moreover, the DNA binding ability of **1** is also stronger than [(phdpa)Cu(bpy)(ClO_4)] (3.69×10^4 M^{-1}) and [(phdpa)Cu(phen)(H_2O)] (8.20×10^4 M^{-1}) [12], which shares similar ligand structure with incorporation of pyridyl instead of quinolyl. The result suggests that, with stronger hydrophobic DNA interaction and larger aromaticity, the incorporation of quinolyl moiety in **L** shows better DNA affinity.

3.2.3. Cleavage of pBR322 DNA by complex without added reagents. To assess the DNA cleavage ability of **1**, supercoiled (SC) pBR322 DNA was incubated with varying concentrations of **1** in a medium of 50 mM Tris–HCl/18 mM NaCl buffer (pH 7.2) for 3 h (figure 5). The cleavage reactions on plasmid DNA by **1** can be monitored by agarose gel electrophoresis. Except a few examples of hydrolytic cleavage, most DNA cleavage agents were mediated by Cu(II) complexes through an oxidative mechanism [25]. Activators [6, 10] or light [26] usually used in the reactions to generate reactive oxygen species (ROS) or reactive metal-oxo species upon reaction with copper limit the development of such metal agents in our body. However, different from reported complexes, **1** shows efficient DNA cleavage without activators. It is clear from figure 5 that at 20 μM **1** converts 50% SC DNA (Form I) into nicked circular NC DNA (Form II) with prominent DNA cleavage. As the concentration of **1** increases, more SC DNA was converted into NC DNA, showing concentration dependence. When the concentration is 35 μM, **1** could completely degrade SC DNA into NC DNA, though LC DNA (Form III) is still not found even at 40 μM. After concentration-dependent DNA cleavage of **1**, it is clear that **1** exhibits self-activated DNA cleavage without activators, which may be conducive for *in vivo* applications.

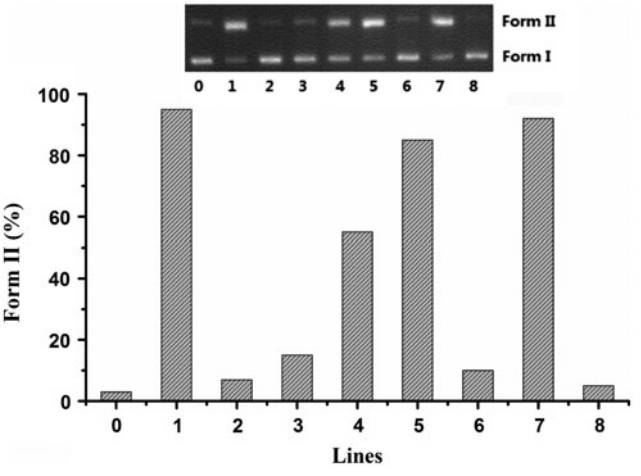

Figure 6. Cleavage of plasmid pBR322 DNA (0.1 μg/μL^{-1}) in the presence of **1** (30 μM) and different inhibitors after 3 h incubation at 37 °C; Line 0: DNA control; Line 1: DNA + **1** (30 μM); Lines 2–10: DNA + **1** + (10 mM KI, 10 mM L-His, 20 μ/mL SOD, 20 μ/mL Catalase, Methyl Green, SYBR Green, 10 mM EDTA).

3.2.4. DNA cleavage mechanism. The activity for DNA cleavage without an oxidant or reducing agent is often related to a hydrolytic rather than oxidative mechanism. However, without a co-reagent, there are still many complexes that act by an oxidative mechanism [8, 27]. In order to diagnose the reactive species responsible for DNA cleavage, the quenching assay was monitored in the presence of different scavengers, and the results are depicted in figure 6. The addition of hydroxyl radical scavenger KI and singlet-oxygen scavengers L-His caused strong inhibition of the nuclease activity, and cleavage ability was also influenced in the presence of $O_2^{\cdot -}$ radical SOD, which indicated that $^{\cdot}OH$ and $^1O_2$ may be the main ROS species in the reaction while $O_2^{\cdot -}$ is also involved in the DNA cleavage [10]. Methyl green and EDTA efficiently inhibit the cleavage, which implies that **1** may bind to DNA in the major groove and metal ions may participate in the cleavage process. In summary, hydroxyl radicals are the crucial ROS responsible for the cleavage activity of **1**; singlet oxygen and $O_2^{\cdot -}$ are less influential in the cleavage.

3.3. *Protein binding activities*

Investigation on the binding of a drug with protein facilitates interpretation of the metabolism and transporting process of a drug and to explain the relationship between structures and functions of protein. BSA was utilized extensively as a result of its structural homology with human serum albumin. Qualitative analysis of binding of compounds to BSA is usually detected by inspecting the fluorescence spectra. BSA consists of three aromatic amino acids (phenylalanine, tyrosine, and tryptophan), and its fluorescence can appear because of tryptophan and tyrosine residues [28]. Figure 7 shows the effect of **1** on the fluorescence intensity of BSA protein.

Upon addition of **1** to solution of BSA, a significant decrease of fluorescence intensity has been observed. The fluorescence intensity of BSA at 350 nm decreased about 58.7% from the initial fluorescence intensity of BSA, which suggested an interaction of the compound with the BSA protein [29]. Quenching mechanisms are usually classified as either

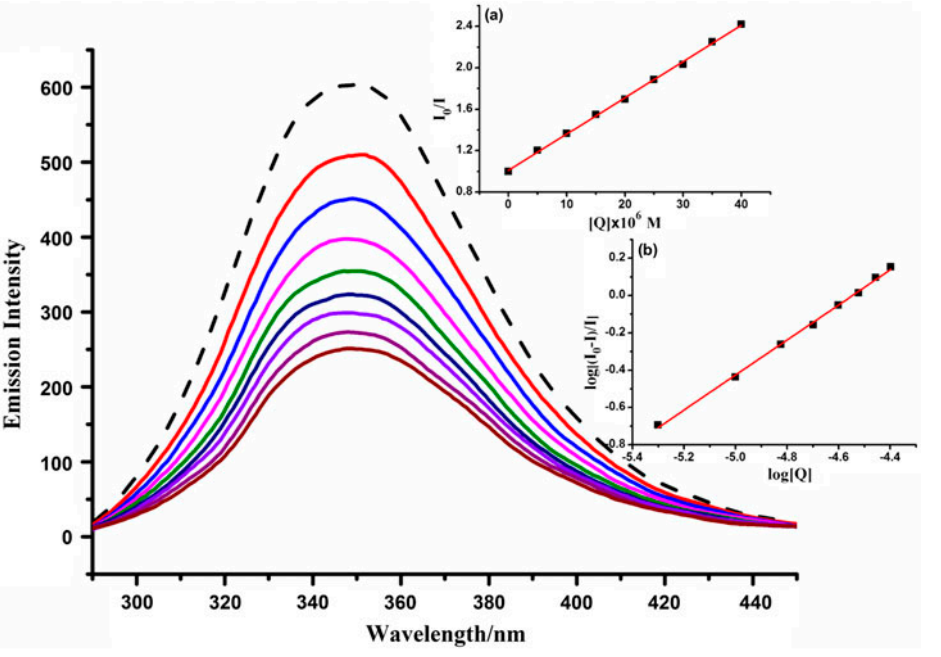

Figure 7. Fluorescence emission spectra of the BSA (29.4 μM) system in the absence (dashed line) and presence (solid lines) of **1** (0–40 μM, respectively). The insets (a) the plot of I_0/I *vs.* the concentration of complex; (b) plot of log $(I_0 - I)$ /I *vs.* log[Q] for BSA in the presence of **1**.

dynamic quenching or static quenching. Static quenching refers to fluorophore−quencher complex formation, and if fluorophore and quencher come into contact during transient existence of the exited state, dynamic quenching happens. To study the quenching process, fluorescence quenching data have been analyzed by the Stern–Volmer equation: $I_0/I = 1 + K_{sv}[Q] = 1 + K_q\tau_0$[Q], where I_0 and I are fluorescence intensities of fluorophore in the absence and presence of quencher, respectively, τ_0 is the average life time of biomolecule without quencher (about 10^{-8} s) and K_{sv} is the Stern–Volmer quenching constant. The plot of I_0/I *versus* [Q] and the Stern–Volmer plots of fluorescence titration data for **1** are shown in figure 7 and table 5. From table 5, the calculated bimolecular quenching rate constants (K_q) were larger than the maximum K_q value of various quenchers to biopolymers (2.0×10^{10} $M^{-1}s^{-1}$) [29], which suggests the formation of BSA-compound complex.

A simple method to explore the quenching mechanism is UV–visible absorption spectroscopy. The electronic spectrum of BSA with **1** is shown in figure 8. In the presence of **1**, the absorption intensity was enhanced which further revealed the static interaction between BSA and **1** [30].

Table 5. The quenching constant, binding constant, and number of binding sites for interaction of **1** with BSA.

Complex **1**	K_{sv} (M^{-1})	K_q (M^{-1} s^{-1})	K (M^{-1})	n
	3.5×10^4	3.5×10^{12}	1.87×10^4	0.94

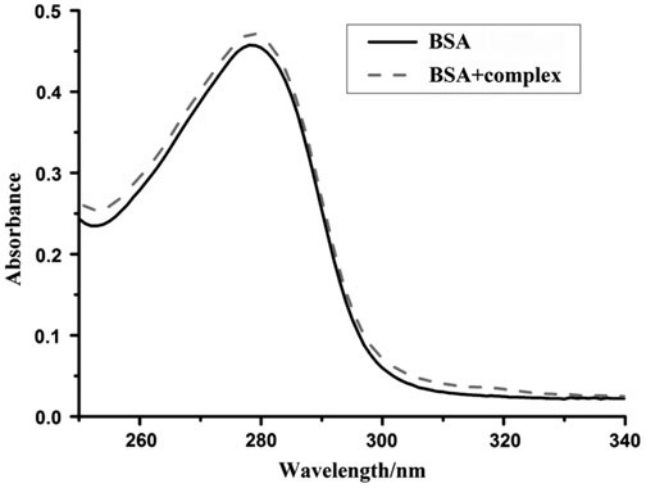

Figure 8. Absorption spectra of BSA (15 μM) and BSA with **1** (1 μM).

For static quenching, if it is assumed that the binding of **1** with BSA could occur at equilibrium, the binding constant (K) could be analyzed by the Scatchard equation:

$$\log[(I_0 - I)/I] = \log K + n \log[Q]$$

where K is the binding constant of the compound with BSA and n is the number of binding sites. The number of binding sites (n) and binding constant (K) have been obtained from the plot of $\log(I_0 - I)/I$ *versus* $\log[Q]$ and are listed in table 5. The K value of **1** is smaller than several reported mononuclear Cu(II) complexes [19, 31], which may be due to large steric effects as a result of the incorporation of phenyl. The value of n is approximately equal to one, which indicates that there is just one independent binding site in BSA for **1**.

3.4. In vitro *cell assay*

The CCK-8 assay was carried out to evaluate the *in vitro* cytotoxicity of **1** against HeLa cells. The CCK-8 assay is a well-established method for determination of cell viability in cell proliferation and cytotoxicity assays [32, 33], which utilizes Dojindo's highly water-soluble tetrazolium salt, WST-8, to produce water-soluble formazan dye on reduction in the living cells to determine the number of living cells. Complex **1** shows prominent cytotoxicity, and the IC_{50} value (2.13 μM) obtained by plotting the cell viability against concentration of **1** reveals that **1** exhibits seven fold cytotoxicity higher than cisplatin (15 μM) [34] for 48 h incubation. Notably, **1** shows prominent cytotoxicity against Hela cells even with incubation for 24 h with IC_{50} of 2.84 μM, which indicates that our complex may be a new candidate for metal-based anticancer agents. However, further investigations should be carried out in order to apply the drug in clinic.

4. Conclusion

With the tridentate polyquinolinyl ligand, bis(2-quinolinyl methyl)benzyl-amine, a new water-soluble Cu(II) complex, has been prepared and characterized by structural and spectral methods. The incorporation of quinoline not only increases the planarity but also the hydrophilic interactions when compared to the reported pyridine analogs, which may contribute to the good DNA binding ability. Further investigations, by absorption and fluorescence measurements, demonstrated that **1** may bind with DNA through partial intercalation. Also, **1** shows good self-activated DNA cleavage ability, offering potential application *in vivo*; complex **1** promotes DNA cleavage in an oxidative way; hydroxyl radical and singlet oxygen may be the main ROS radicals in the process. According to the results obtained from fluorescence and UV–visible spectrometry, we speculate that **1** could bind with BSA in a static quenching process. Complex **1** shows a considerable cytotoxic activity (IC_{50} = 2.84 μM) against Hela cells, better than cisplain, which suggests that **1** may be a potential anticancer drug.

Funding

This work was supported by the National Natural Science Foundation of China [grant number 21171101], [grant number 21371103], [grant number 21471085]; Tianjin Science Foundation [grant number 12JCYBJC13600]; NFFTBS [grant number J1103306]; MOE Innovation Team [grant number IRT13022] of China.

References

[1] G. Barone, A. Terenzi, A. Lauria, A.M. Almerico, J.M. Leal, N. Busto, B. García. *Coord. Chem. Rev.*, **257**, 2848 (2013).
[2] B. Rosenberg, L. Vancamp, J. Trosko, V. Mansour. *Nature*, **222**, 385 (1969).
[3] E.S. Antonarakis, A. Emadi. *Cancer Chemother. Pharmacol.*, **66**, 1 (2010).
[4] B.M. Zeglis, V.C. Pierre, J.K. Barton. *Chem. Commun.*, 4565 (2007).
[5] P.P. Silva, W. Guerra, G.C. dos Santos, N.G. Fernandes, J.N. Silveira, A.M. da Costa Ferreira, T. Bortolotto, H. Terenzi, A.J. Bortoluzzi, A. Neves, E.C. Pereira-Maia. *J. Inorg. Biochem.*, **132**, 67 (2014).
[6] C. Rajarajeswari, R. Loganathan, M. Palaniandavar, E. Suresh, A. Riyasdeen, M.A. Akbarsha. *Dalton Trans.*, **42**, 8347 (2013).
[7] K. Ghosh, P. Kumar, V. Mohan, U.P. Singh, S. Kasiri, S.S. Mandal. *Inorg. Chem.*, **51**, 3343 (2012).
[8] P.U. Maheswari, S. Roy, H. den Dulk, S. Barends, G. van Wezel, B. Kozlevčar, P. Gamez, J. Reedijk. *J. Am. Chem. Soc.*, **128**, 710 (2006).
[9] C. Santini, M. Pellei, V. Gandin, M. Porchia, F. Tisato, C. Marzano. *Chem. Rev.*, **114**, 815 (2014).
[10] W. Zhou, X. Wang, M. Hu, Z.J. Guo. *J. Inorg. Biochem.*, **121**, 114 (2013).
[11] M. Kruppa, B. König. *Chem. Rev.*, **106**, 3520 (2006).
[12] Q.Y. Chen, H.J. Fu, W.H. Zhu, Y. Qi, Z.P. Ma, K.D. Zhao, J. Gao. *Dalton Trans.*, **40**, 4414 (2011).
[13] V.R.L. Solomon, H. Lee. *Curr. Med. Chem.*, **18**, 1488 (2011).
[14] H. Kim, J. Kang, K.B. Kim, E.J. Song, C. Kim. *Spectrochim. Acta, Part A*, **118**, 883 (2014).
[15] G.M. Sheldrick. *SHELXS-97, Program for the Solution of Crystal Structure, Program for the Refinement of Crystal Structure*. University of Gottingen, Germany (1997).
[16] J. Marmur. *J. Mol. Biol.*, **3**, 208 (1961).
[17] F.B. Tamboura, M. Gaye, A.S. Sall, A.H. Barry, T. Jouini. *Inorg. Chem. Commun.*, **5**, 235 (2002).
[18] B. Antonioli, B. Büchner, J.K. Clegg, K. Gloe, K. Gloe, L. Götzke, A. Heine, A. Jäger, K.A. Jolliffe, O. Kataeva, V. Kataev, R. Klingeler, T. Krause, L.F. Lindoy, A. Popa, W. Seichter, M. Wenzel. *Dalton Trans.*, 4795 (2009).
[19] D.S. Raja, N.S.P. Bhuvanesh, K. Natarajan. *Inorg. Chem.*, **50**, 12852 (2011).
[20] Z.C. Liu, B.D. Wang, Z.Y. Yang, Y. Li, D.D. Qin, T.R. Li. *Eur. J. Med. Chem.*, **44**, 4477 (2009).
[21] M.T. Carter, M. Rodriguez, A.J. Bard. *J. Am. Chem. Soc.*, **111**, 8901 (1989).
[22] J. Lu, Q. Sun, J.L. Li, L. Jiang, W. Gu, X. Liu, J.L. Tian, S.P. Yan. *J. Inorg. Biochem.*, **137**, 46 (2014).
[23] S. Saha, R. Majumdar, M. Roy, R.R. Dighe, A.R. Chakravarty. *Inorg. Chem.*, **48**, 2652 (2009).
[24] Y.B. Zeng, N. Yang, W.S. Liu, N. Tang. *J. Inorg. Biochem.*, **97**, 258 (2003).
[25] C. Liu, M. Wang, T. Zhang, H. Sun. *Coord. Chem. Rev.*, **248**, 147 (2004).

[26] G.J. Chen, X. Qiao, P.Q. Qiao, G.J. Xu, J.Y. Xu, J.L. Tian, W. Gu, X. Liu, S.P. Yan. *J. Inorg. Biochem.*, **105**, 119 (2011).
[27] P.P. Silva, W. Guerra, J.N. Silveira, A.M. da C. Ferreira, T. Bortolotto, F.L. Fischer, H. Terenzi, A. Neves, E.C. Pereira-Maia. *Inorg. Chem.*, **50**, 6414 (2011).
[28] O.K. Abou-Zied, O.I.K. Al-Shihi. *J. Am. Chem. Soc.*, **130**, 10793 (2008).
[29] A. Patra, T.K. Sen, A. Ghorai, G.T. Musie, S.K. Mandal, U. Ghosh, M. Bera. *Inorg. Chem.*, **52**, 2880 (2013).
[30] Y.J. Hu, O.Y. Yu, C.M. Dai, Y. Liu, X.H. Xiao. *Biomacromolecules*, **11**, 106 (2010).
[31] X.F. Zhao, O.Y. Yan, Y.Z. Liu, Q.J. Su, H. Tian, C.Z. Xie, J.Y. Xu. *New J. Chem.*, **38**, 955 (2014).
[32] M. Liong, J. Lu, M. Kovochich, T. Xia, S.G. Ruehm, A.E. Nel, F. Tamanoi, J.I. Zink. *ACS Nano*, **2**, 889 (2008).
[33] L. Yuan, W.L. Chen, J. Hu, J.Z. Zhang, D. Yang. *Langmuir*, **29**, 734 (2013).
[34] R.W.Y. Sun, A.L.F. Chow, X.H. Li, J.J. Yan, S.S.Y. Chui, C.M. Che. *Chem. Sci.*, **2**, 728 (2011).